CANCER GENOMICS & PROTEOMICS *14*: 409-425 (2017)
doi:10.21873/cgp.20051

Transcriptomic Profiling of MDA-MB-231 Cells Exposed to *Boswellia Serrata* and 3-O-Acetyl-B-Boswellic Acid; ER/UPR Mediated Programmed Cell Death

ELIZABETH A. MAZZIO, CHARLES A. LEWIS and KARAM F.A. SOLIMAN

College of Pharmacy & Pharmaceutical Sciences, Florida A & M University, Tallahassee, FL, U.S.A.

Abstract. *Background/Aim: Triple-negative breast cancer (TNBC) is characterized by the absence of hormone receptors (estrogen, progesterone and human epidermal growth factor receptor-2) and a relatively poor prognosis due to inefficacy of hormone receptor-based chemotherapies. It is imperative that we continue to explore natural products with potential to impede growth and metastasis of TNBC. In this study, we screened over 1,000 natural products for capacity to induce cell death in TNBC (MDA-MB -231) cells. Materials and Methods: Frankincense (Boswellia serrata extract (BSE)) and 3-O-Acetyl-β-boswellic acid (3-OAβBA) were relatively potent, findings that corroborate the body of existing literature. The effects of BSE and 3-OAβBA on genetic parameters in MDA-MB-231 cells were evaluated by examining whole-transcriptomic influence on mRNAs, long intergenic non-coding RNA transcripts (lincRNA) and non-coding miRNAs. Results: Bio-statistical analysis demarcates the primary effect of both BSE/3-OAβBA on the up-regulation of PERK (protein kinase RNA-like endoplasmic reticulum kinase)– endoplasmic reticulum (ER)/unfolded protein response (UPR) pathways that are closely tied to activated programmed cell death (APCD). Global profiling confirms concomitant effects of BSE/3-OAβBA on upwardly expressed ER/URP APCD key components PERK (EIF2AK3), XBP1, C/EBP homologous protein transcription factor (CHOP), ATF3 and DDIT3,4/DNA-damage-inducible transcript 3,4 (GADD34). Further, BSE and/or 3-OAβBA significantly down-regulated oncogenes (OG) which, heretofore, lack functional pathway mapping, but are capable of driving epithelial–mesenchymal transition (EMT), cell survival, proliferation, metastasis and drug resistance. Among these are cell migration-inducing protein hyaluronan binding (CEMIP) [–7.22]; transglutaminase 2 [–4.96], SRY box 9 (SOX9) [–4.09], inhibitor of DNA binding 1, dominant negative helix-loop-helix protein (ID1) [–6.56]; and endothelin 1 (EDN1, [-5.06]). Likewise, in the opposite manner, BSE and/or 3-OAβBA induced the robust overexpression of tumor suppressor genes (TSGs), including: glutathione-depleting ChaC glutathione-specific gamma-glutamylcyclotransferase 1 (CHAC1) [+21.67]; the mTOR inhibitors - sestrin 2 (SESN2) [+16.4] Tribbles homolog 3 (TRIB3) [+6.2], homocysteine-inducible, endoplasmic reticulum stress-inducible, ubiquitin-like domain member 1 (HERPUD1) [+12.01]; and cystathionine gamma-lyase (CTH) [+11.12]. Conclusion: The anti-cancer effects of the historically used frankincense sap (BSE) appear to involve major impact on the ER/UPR response, concomitant to effecting multiple targets counter to the growth, proliferation and metastasis of TNBC cancer cells. The microarray data are available at Expression Omnibus GEO Series accession number GSE102891.*

This article is freely accessible online.

Correspondence to: Prof. Karam F.A. Soliman Professor & RCMI Program Director, College of Pharmacy & Pharmaceutical Sciences, Florida A&M University, Room 104 Dyson Pharmacy Building, 1520 ML King Blvd, Tallahassee, FL 32307, U.S.A. Tel: +1 8505993306, Fax: +1 8505993667, e-mail: karam.soliman@famu.edu

Key Words: Boswellic acid, Boswellia, apoptosis, Frankincense, cancer, microarray, endoplasmic reticulum, UPR, CHOP, ATF, ER, PERK, CHAC1, SESN2, TG2, sestrin, dual specificity phosphatase, histone cluster, epigenetics.

Frankincense has been used as a valuable multi-purpose natural product for over 5,000 years, where its medicinal form is derived from the tree sap resin of diverse species from the genus *Boswellia*/family *Burseraceae*. Its extended historical use reflects valuable insight about its properties from our ancestors who had a greater dependency on natural medicines. In the past century, with the rapid development of synthetic medicines, botanical therapeutics are perceived as menial compared to that of current medical treatment. Yet, at the same time, scientific literature continues to report *Boswellia* and its active component: boswellic acid can exert

diverse antitumor properties (1) with the capacity to attenuate proliferation, angiogenesis, invasion and metastasis in established models (2-7).

With the availability of current biotechnologies, it is evident that *Boswellia* can mediate anti-cancer effects through direct reduction of pro-oncogenic proteins and transcription factors that otherwise drive aggressive malignancies. Just for a few examples, *Boswellia* and its constituents suppress NF-κB, Bcl-2, bcl-xL, Mcl-1, IAP-1, BIRC5, VEGF (2, 8, 9) mPGES-1, MMP-2,7,9, PGE2 (5) cyclin D1, PCNA, c-Myc (10), cyclin E, CDK 2 and 4 and retinoblastoma (Rb) (11). Central to these effects are control over STAT3 phosphorylation of Jak 2/Src or Akt/GSK3β signaling tantamount to triggering apoptotic pathways through caspase-9, caspase-3, and cleaved PARP (12, 13). Other reported anti-cancer attributes of *Boswellia* include its potential to block the development of chemically induced cancers such as that by azomethane (14), prevent multidrug resistance (15) and act as a chemo-sensitizing agent (4, 16). These effects are consistently observed both in *in vitro* and *in vivo* (10). With regards to triple negative breast cancer (TNBC), *Boswellia serrata* extract (BSE) and 3-O-Acetyl-β-boswellic acid (3-OAβBA) are equally effective against its growth and that of other malignant breast tumor cell lines (8, 17, 18).

Here, we further investigate precipitating transcriptome changes induced by *Boswellia serrata* extract and 3-OAβBA, in order to determine the major cause of cell death in TNBC breast cancer cells. These findings can serve as a general directive in future studies investigating the anti-cancer properties of frankincense.

Materials and Methods

Hanks Balanced Salt Solution, (4-(2-hydroxyethyl)-1-piperazine-ethanesulfonic acid) (HEPES), absolute ethanol ≥99.8%, 96 well plates, pipette tips, Dulbecco's modified Eagle's medium (DMEM), fetal bovine serum (FBS), penicillin/streptomycin general reagents and supplies were all purchased from Sigma-Aldrich Co. (St. Louis, MO, USA) and VWR International (Radnor, PA, USA). Triple-negative human breast tumor (MDA-MB-231) cells were obtained from the American Type Culture Collection (Rockville, MD, USA). *Boswellia serrata* was obtained from Starwest Botanicals (Sacramento, CA, USA) and 3-O-Acetyl-β-boswellic acid was purchased from Cayman Chemical (Ann Arbor, MI, USA). All microarray equipment, reagents and materials were purchased from Affymetrix/ Thermo Fisher (Waltham, MA, USA).

All natural chemicals, reference drugs and (3-OAβBA) were dissolved in DMSO [5-20 mg/mL], where the crude herbs including *Boswellia serrata* were prepared in absolute ethanol [50 mg/mL] after being diced, macerated and powdered prior to being stored at –20˚C. All dilutions were prepared in sterile HBSS + 5 mM HEPES, adjusted to a pH of 7.4, ensuring solvent concentration of DMSO or absolute ethanol at less than 0.5%.

Cell culture. MDA-MB-231 cells were cultured in 175 cm^2 flasks containing DMEM supplemented with 10% FBS and 100 U/ml penicillin G sodium/100 μg/ml streptomycin sulfate. Cells were grown at 37˚C in 5% CO_2/atmosphere and sub-cultured every three to five days.

Cell viability assay. Alamar Blue cell viability assay was used to determine cytotoxicity. Viable cells are capable of reducing resazurin to resorufin (a detectable fluoroprobe). Briefly, 96-well plates were seeded with MDA-MB-231 cells at a density of 5×10^6 cells/ml. Cells were treated with HBSS (control) and various concentrations of *Boswellia serrata* extract or 3-O-Acetyl-β-boswellic acid for 24 h at 37˚C, 5% CO_2 in atmosphere. Alamar blue (0.1 mg/ml in HBSS) was added at 15% v/v to each well, and the plates were incubated for 6-8 h. Quantitative analysis of dye conversion was measured on a Synergy™ HTX Multi-Mode microplate reader (BioTek, Winooski, VT, USA), 550nm /580nm (excitation/emission). The data were expressed as a percentage of untreated controls.

Fluorescence microscopy. Live cell imaging was conducted using Fluorescein diacetate (FDA), which is a cell-permeable esterase substrate. The fluorescein molecule accumulates in cells that possess intact membranes, serving as a marker of cell viability. Briefly, FDA was dissolved in ethanol 4.2 mg/ml and subsequently prepared at 20 μM in HBSS. After 30 min of incubation, samples were analyzed photographically using a fluorescent /inverted microscope, CCD camera and data acquisition by ToupTek View (ToupTek Photonics Co, Zhejiang, P.R. China).

Microarray WT 2.1 human datasets. After treatment, cells were washed three times in HBSS, rapidly frozen and stored at –80˚C. Total RNA was isolated/ purified using the TRIzol/chloroform method, quality was assessed and concentration was equalized to 82 ng/μl in nuclease free water. Whole transcriptome analysis was conducted according to the GeneChip™ WT PLUS Reagent Manual for Whole Transcript (WT) Expression Arrays. Briefly, RNA was synthesized to first strand cDNA, second-strand cDNA, followed by transcription to cRNA. cRNA was purified and assessed for yield, prior to 2nd cycle single stranded cDNA synthesis, hydrolysis of RNA and purification of 2nd cycle single stranded cDNA. cDNA was then quantified for yield and equalized to 176 ng/ml. Subsequently, cDNA was fragmented, labeled and hybridized on to the arrays prior to being subjected to fluidics and imaging using the Gene Atlas (Affymetrix, ThermoFisher Scientific, Waltham, MA, USA).

The array data quality control and initial processing from CEL to CHP files were conducted using expression console, prior to data evaluation using the Affymetrix transcriptome analysis console. Supportive analysis was accomplished using geneontology.org (19) and DAVID Bioinformatics Resources 6.8 National Institute of Allergy and Infectious Diseases (NIAID), NIH (20).

Microarray miRNA 4.1 human datasets. miRNA was isolated using the QIAzol reagent and miRNeasy Mini Kit (Qiagen, Germantown, MD). Briefly, after RNA purification, samples were labeled with a POLY A tail, and ligated using a flash tag ligation mix from the FlashTag™ Biotin HSR RNA kit (Affymetrix). Subsequently, biotin labeled RNA was detected using streptavidin – EP and hybridized onto a Genechip miRNA 4.1 human array, prior to fluidics and imaging by the Gene Atlas. The array data quality control and initial processing from CEL to CHP files were conducted using expression console, prior to data evaluation using the transcriptome analysis console provided

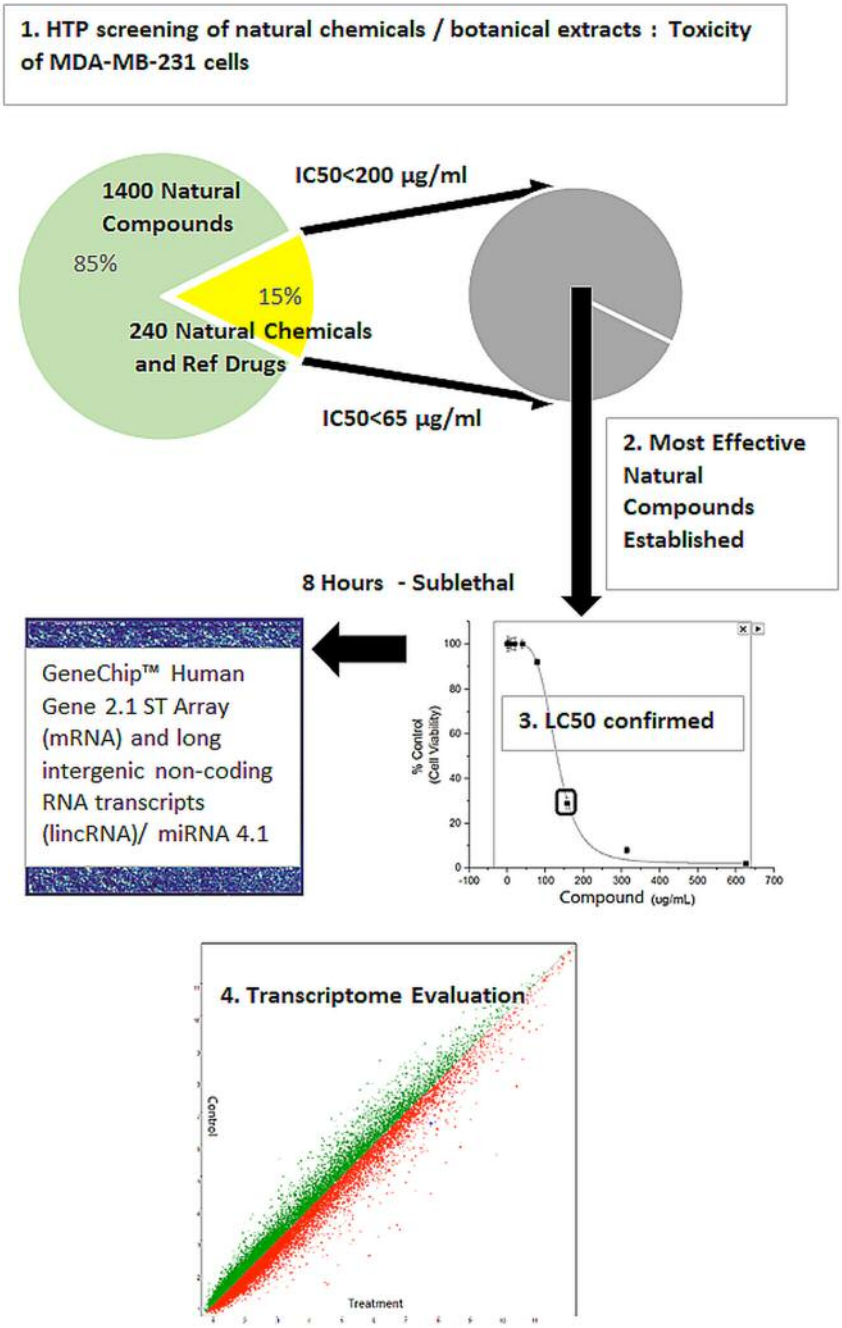

Figure 1. *Natural compound screening procedure: A total of 240 in -house natural plant-derived chemicals (<65 µg/ml) and 1,400 botanical herbs (<200 µg/ml) were tested for capacity to induce cytotoxicity on MDA-MB-231 cells, relative to chemotherapy drugs. Lead compounds Frankincense (Boswellia serrata extract (BSE)) and 3-O-Acetyl-β-boswellic acid (3-OAβBA) were then cultured for 8 hours at the LC_{50}, prior to cell death – and immediately frozen at –80˚C. Microarray analysis was performed to identify biological influence on the entire transcriptome.*

by Affymetrix. Supportive analysis was accomplished using geneontology.org (19) and DIANA miRPath tools (21, 22).

Data analysis. Statistical analysis was performed using Graph Pad Prism (version 3.0; Graph Pad Software Inc. San Diego, CA, USA) with significance of difference between the groups assessed using a one-way ANOVA, then followed by a Tukey post hoc means comparison test, or a Student's *t*-test. LC_{50}s were determined by regression analysis using Origin Software (Origin Lab, Northampton, MA, USA).

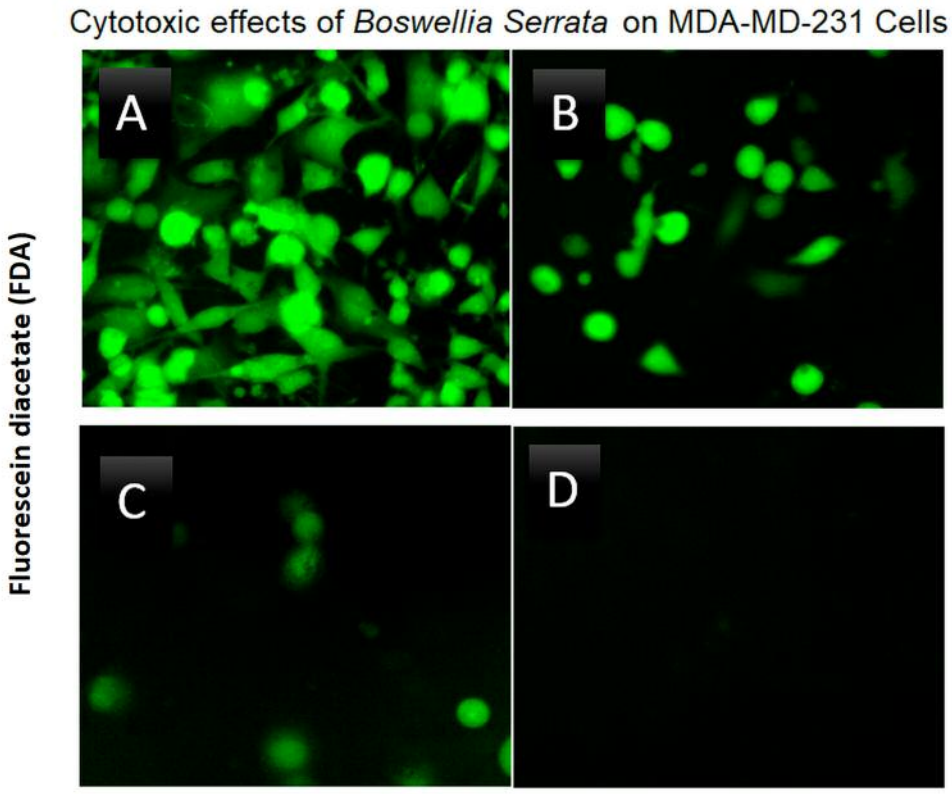

Figure 2. *Cytotoxic effects of Boswellia serrata (BSE) on MDA-MB-231 cells at 24 h of incubation at 37˚C, 5% CO_2/Atm. The data reflect loss of cell viability using FDA which is cleaved only by viable cells. (A) Untreated Control (B) 156 μg/ml (C) 313 μg/ml (D) 626 μg/ml.*

Results

A high throughput (HTP) screening module is routinely used in our facility to enable the preliminary evaluation of thousands of herbs and plant chemicals on selective targets, and in this case for relative capacity to induce cell death in MDA-MB-231 cells (Figure 1). Briefly, LC_{50}s were established, natural products were ranked for potency and lead compounds identified. Here we focus on the natural herb: *Boswellia serrata* (BSE), where we present fluorescence FDA staining showing a loss of viability over concentration (Figure 2) and corresponding cytotoxicity as determined by Alamar Blue (Figure 3). The LC_{50}s were determined (128.8 μg/ml) for BSE and its active component 3-OAβBA (46.32 μg/ml) (Figure 4).

For whole transcriptome microarray studies, the LC_{50}s of BSE and 3-OAβBA were applied to fully viable cells at Time 0 (zero minutes), and morphological changes were monitored every hour, to ensure no cell death was evident. At 6-8 h, the cells retained morphological shape, flask attachment and had no obvious signs of cell death. At this point, cells were rapidly washed in HBSS 3x, spun and frozen at –80˚C. This time of acquisition was ascertained as appropriate to ensure capture of information on pivotal events elicited/precipitating cell death.

Using affymetrix human whole transcriptome arrays [GeneChip Human Gene Array 2.1], the data showed that of the 48226 transcripts tested, there were 300 differentially expressed genes (DEGs) for BSE (265 up-regulated/65 down-regulated) and for 3-OAβBA: 931 DEGs (391 up-regulated/540 down-regulated). An overview of the transcriptome data for BSE treatment are presented by a volcano plot (Figure 5) showing fold change (FC) *vs.* significance – then cross referenced to Table I, which presents the largest differentially expressed changes. An overview of microarray data for 3-OAβBA treatments are presented by a similar volcano plot (Figure 6) also cross referenced to Table II, showing the largest differentially expressed changes. The data discussed in this publication have been deposited in NCBI's Gene Expression Omnibus and are accessible through GEO Series accession number GSE102891 located at https://www.ncbi.nlm.nih.gov/geo/query/acc.cgi?acc=GSE102891.

The pathway of greatest impact for both BSE and 3-OAβBA elucidated by the Affymetrix transcriptome analysis console, sorted by greatest relevance was up up-regulation of the photodynamic therapy unfolded protein response (Figure 7).

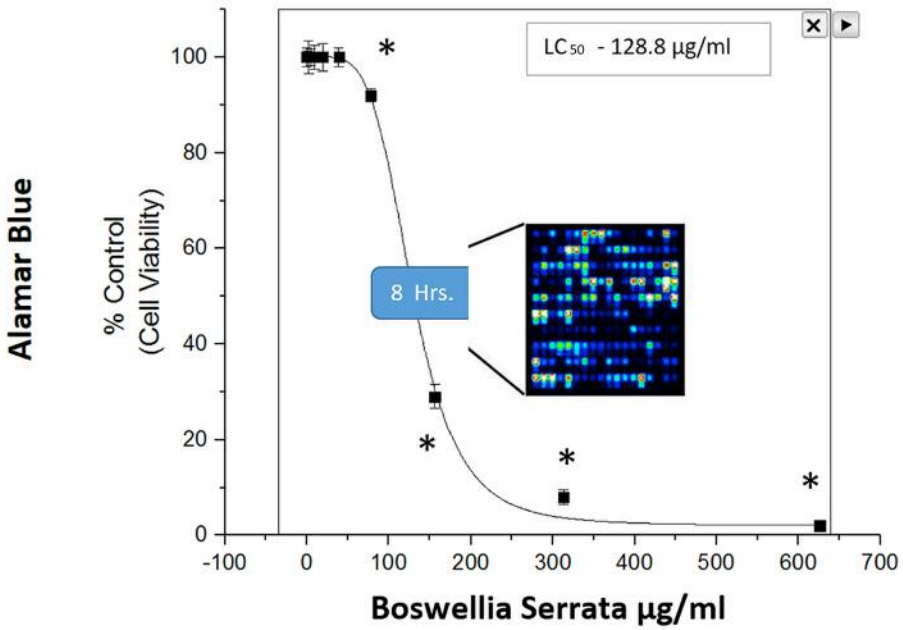

Figure 3. *Cytotoxicity of BSE on MDA-MB-231 cells at 24 h of incubation at 37˚C, 5% CO_2/Atm. The data represent loss of viability as % control values as determined with Alamar Blue assay. The data are presented as the Mean±S.E. M, n=4, and significant difference from the controls were determined by a one-way ANOVA followed by a Tukey post hoc comparison test, *p<0.05.*

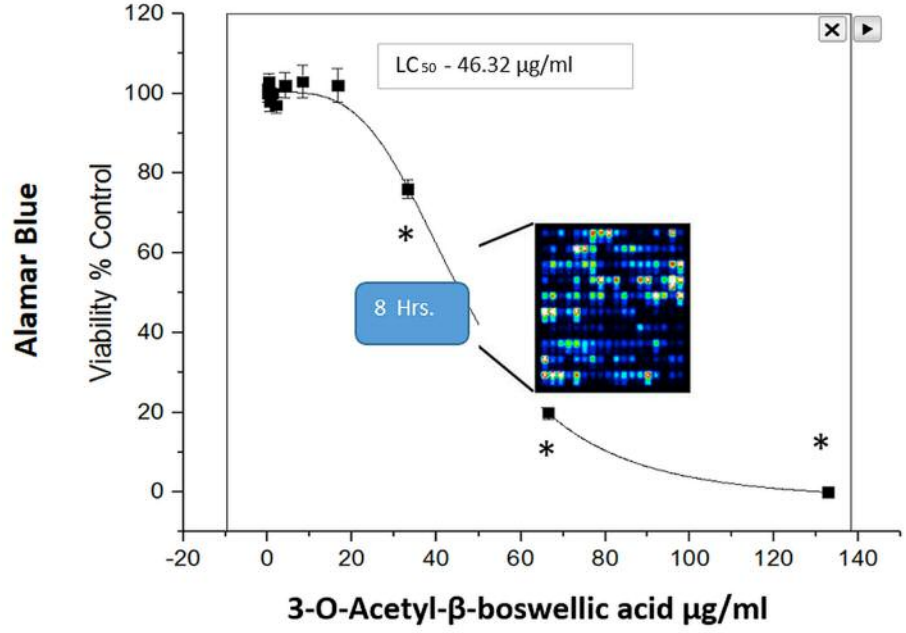

Figure 4. *Cytotoxicity of 3-OAβBA on MDA-MB-231 cells at 24 h of incubation at 37˚C, 5%CO_2/Atm. The data represent loss of viability as % Control values as determined with Alamar Blue assay. The data are presented as the mean±S.E. M, n=4, and significant differences from the controls were determined by a one-way ANOVA followed by a Tukey post-hoc comparison test, *p<0.05.*

Using DAVID Functional Annotation Bioinformatics Microarray Analysis (20), we also found that the endoplasm reticulum was largely affected – up-regulated genes are shown on a KEGG overlay pathway map (Figure 8). Again, there was a very close overlay between BSE and 3-OAβBA to elicit these ER mediated responses. In terms of dataset analysis for

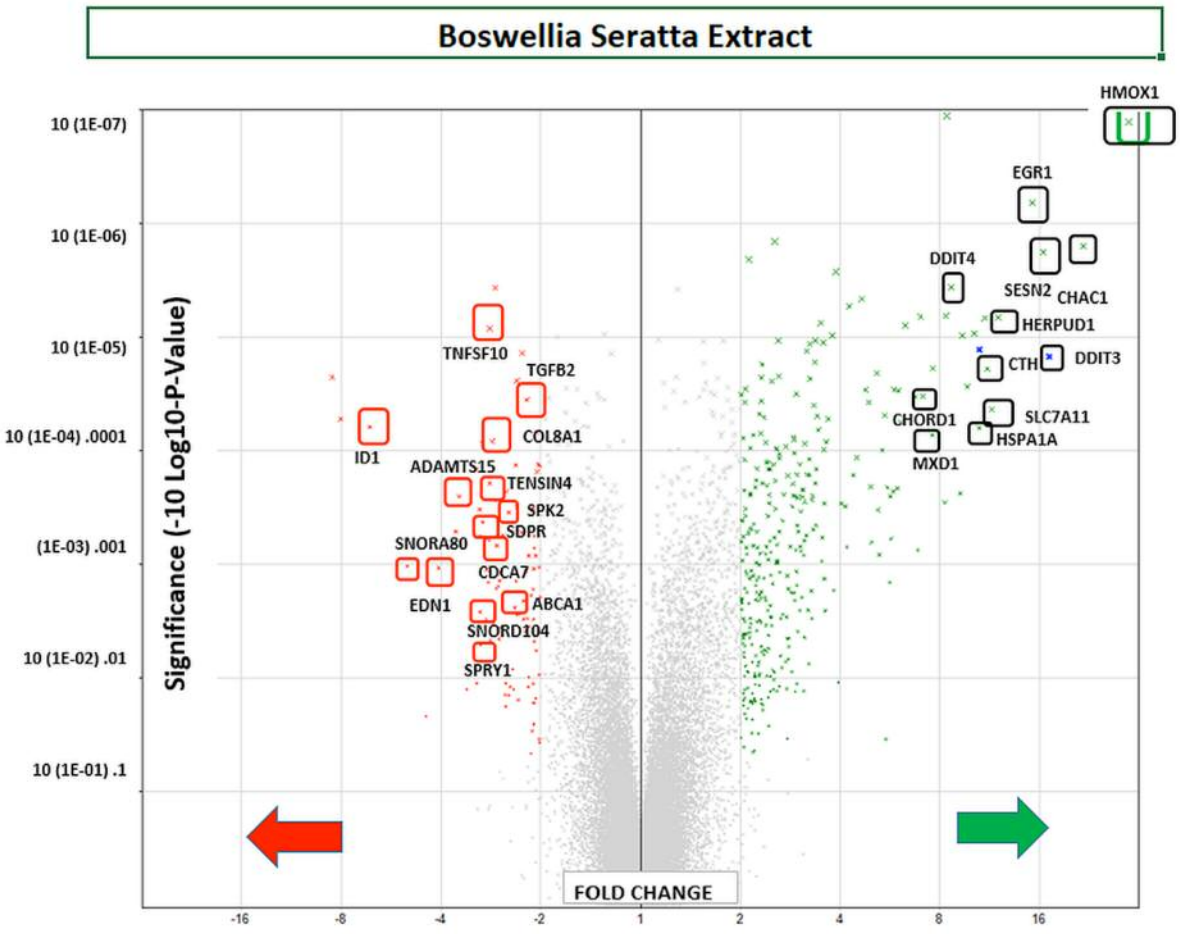

Figure 5. *WT changes in BSE treated cells using GeneChip™ Human Gene 2.1 ST Array. 48226 transcripts were tested, 300 differentially expressed genes (DEGs) were identified for (265 up-regulated/65 down-regulated). The data are presented by a volcano plot (fold-change by significance) for whole transriptome changes in BSE treated MDA-MB-231 cells vs. controls, n=3. The left panel shows down-regulated genes (red)/right panel (green) shows up-regulated genes: highlighting some of the highest differential changes, also listed in Table I.*

functional biological relevance, we used geneontology.org enrichment analysis tool, which also confirms the findings from Affymetrix and David bio analytic tools, corroborating uniform up-regulation on the ER stress, unfolded protein responses as well as glucose depletion/starvation (Tables III and IV). Interestingly, very few changes were reported for the miRNAs, with reported pathways for hsa-miR-34b-3p (target of 14 genes) and hsa-miR-184 (target of 6 genes), as presented in Table V. These findings provide an overview of *Boswellia* seratta and its pharmacologically active compound, boswellic acid on the transcriptome of TNBCs.

Discussion

The data in this study suggest a primary mode of cell death by 3-OAβBA and BSE to involve ER stress leading to a UPR (unfolded protein response), this commonly associated with activated cell death. There has been a recent surge in research describing the importance of the ER/UPR in a variety of human pathologies, many of these relevant to cancer (23-25).

A literature review of the ER/UPR involvement in cancer unveils a scientific uncertainty and need for answers as to why activation of ER/UPR creates a double-edged sword. On the one hand, ER stress inducers (*e.g.* hypoxia, glucose, nutrient deprivation (26, 27) activate the ER/UPR which leads to tumor adaptation (a persistent elevation of pro-survival proteins, a resistance to chemotherapy, greater tumor progression, angiogenesis, invasion and thriving of dormant stem cells (28-30). Yet at the same time, activation of main pathways in the ER/UPR an also trigger programmed cell death (PCD) evidenced by many natural anti-cancer agents (31-41) alkylating/ platinum based drugs and anti-cancer steroids (42-47). Several articles have expressed the need for

Table I. *Greatest transcriptome shifts incurred by BSE in MDA-MB-231 cells. The data represents signal, fold-change, p-Value, gene symbol and gene description. Top mRNA Changes: Affymetrix Microarray WT Human 2.1 ST*

Transcript	BSE	Control	Fold	ANOVA	Gene	Gene
Cluster ID	Bi-weighted AVE Signal Log2	Bi-weighted AVE Signal Log2	Change	*p*-Value	Symbol	Description
16929562	9.61	4.71	29.8	<0.0001	HMOX1	heme oxygenase 1
16799739	8.54	4.1	21.67	<0.0001	CHAC1	ChaC glutathione-specific gamma-glutamylcyclotransferase 1
16766578	6.53	2.44	17.09	<0.0001	DDIT3	DNA damage-inducible transcript 3 protein
16661544	8.05	4.02	16.4	<0.0001	SESN2	Sestrin 2
16989736	8.02	4.1	15.18	<0.0001	EGR1	Early growth response 1
16819325	9.53	5.95	12.01	<0.0001	HERPUD1	Homocysteine-inducible, ER stress-inducible, ubiquitin-like DM1
16979917	10.54	7.02	11.47	<0.0001	SLC7A11	Solute carrier family 7 (anionic at light chain, xc- system), M 11
16666055	7.26	3.78	11.12	<0.0001	CTH	Cystathionine gamma-lyase
16766588	4.98	1.59	10.54	<0.0001	MIR616	MicroRNA 616; DNA-damage-inducible transcript 3
17006863	10.83	7.44	10.51	0.0001	HSPA1A	Heat shock 70kDa protein 1A; heat shock 70kDa protein 1B
17006881	10.92	7.65	9.68	<0.0001	HSPA1B	Heat shock 70kDa protein 1B; heat shock 70kDa protein 1A
16756202	8.57	5.37	9.2	0.0002	EID3	EP300 interacting inhibitor of differentiation 3
16705961	8.87	5.8	8.41	<0.0001	DDIT4	DNA damage inducible transcript 4
16949264	5.58	2.53	8.28	0.0003	LOC344887	NmrA-like family domain containing 1 pseudogene
16881138	7.53	4.61	7.6	<0.0001	MXD1	MAX dimerization protein 1
16743222	8.18	5.35	7.11	<0.0001	CHORDC1	Cysteine and histidine rich domain containing 1
17083614	6.2	3.42	6.85	0.0008	LURAP1L	Leucine rich adaptor protein 1-like
16998044	6.5	3.75	6.73	<0.0001	LUCAT1	Lung cancer associated transcript 1 (non-protein coding)
16910609	7.81	5.16	6.28	<0.0001	TRIB3	Tribbles pseudokinase 3
16974968	6.03	3.42	6.1	0.0001	SEL1L3	Sel-1 suppressor of lin-12-like 3 (*C. elegans*)
17060061	7.75	5.16	6.01	<0.0001	ASNS	Asparagine synthetase (glutamine-hydrolyzing)
16739208	8.05	5.48	5.95	0.0002	FTH1	Ferritin, heavy polypeptide 1
16705551	5.5	2.96	5.82	<0.0001	HKDC1	Hexokinase domain containing 1
16748304	6.07	3.54	5.78	0.0002	GABARAPL1	GABA(A) receptor-associated protein like 1
16772172	6.22	3.71	5.69	0.0006	RPS27A	Ubiquitin C; ribosomal protein S27a
17050328	6.4	3.9	5.65	0.0003	DNAJB9	DnaJ (Hsp40) homolog, subfamily B, member 9
16927633	6.45	3.98	5.55	0.0002	SDF2L1	Stromal cell-derived factor 2-like 1
16859795	6.87	4.43	5.45	<0.0001	GDF15	Growth differentiation factor 15
16700911	4.51	2.09	5.35	0.0001	ERO1B	Endoplasmic reticulum oxidoreductase beta
17024448	8.06	5.66	5.25	0.0008	FBXO30	F-box protein 30
16756209	4.83	2.45	5.2	0.0003	LOC105369949	Uncharacterized LOC105369949
16871000	5.49	3.12	5.16	<0.0001	LINC00662	Long intergenic non-protein coding RNA 662
16800301	5.69	3.38	4.95	0.0002	PDIA3	Protein disulfide isomerase family A member 3
16984032	6.33	7.85	–2.85	0.0002	SKP2	S-phase kinase-associated protein 2, E3 ubiquitin protein ligase
16677071	4.39	5.9	–2.86	0.0006	SERTAD4	SERTA domain containing 4
17075529	3.58	5.12	–2.91	0.0011	ENTPD4	Ectonucleoside triphosphate diphosphohydrolase 4
16725041	6.74	8.29	–2.92	0.0031	FAM111B	Family with sequence similarity 111, member B
16887840	3.79	5.37	–2.99	0.0004	CDCA7	Cell division cycle associated 7
17003249	3.01	4.6	–3	0.0001	PRR7-AS1	PRR7 antisense RNA 1
16696533	5.04	6.63	–3.03	0.0052	SNORD75	Small nucleolar RNA, C/D box 75
16970435	3.09	4.7	–3.04	0.0006	SPRY1	Sprouty RTK signaling antagonist 1
16906615	3.76	5.37	–3.05	0.0003	SDPR	Serum deprivation response
16837061	5.42	7.03	–3.05	0.0026	SNORD104	Small nucleolar RNA, C/D box 104
16844356	4.78	6.42	–3.13	0.0001	TNS4	tensin 4
16733516	3.75	5.57	–3.52	0.0003	ADAMTS15	ADAM metallopeptidase with thrombospondin type 1 motif 15
16925023	3.28	5.31	–4.07	0.0011	SNORA80A	Small nucleolar RNA, H/ACA box 80A
17004903	3.47	5.81	–5.06	0.0010	EDN1	Endothelin 1
16912362	4.56	7.27	–6.56	0.0001	ID1	Inhibitor of DNA binding 1, dominant Negative helix-loop-helix protein

further understanding of the pro-survival/pro-death ER/UPR processes and the relevance timing on cancer initiation, progression and treatment (48). It is believed that if we can further understand control of ER stress regulators on cancer growth, we can successfully use this information to overcome acquired resistance to (49) and augment existing

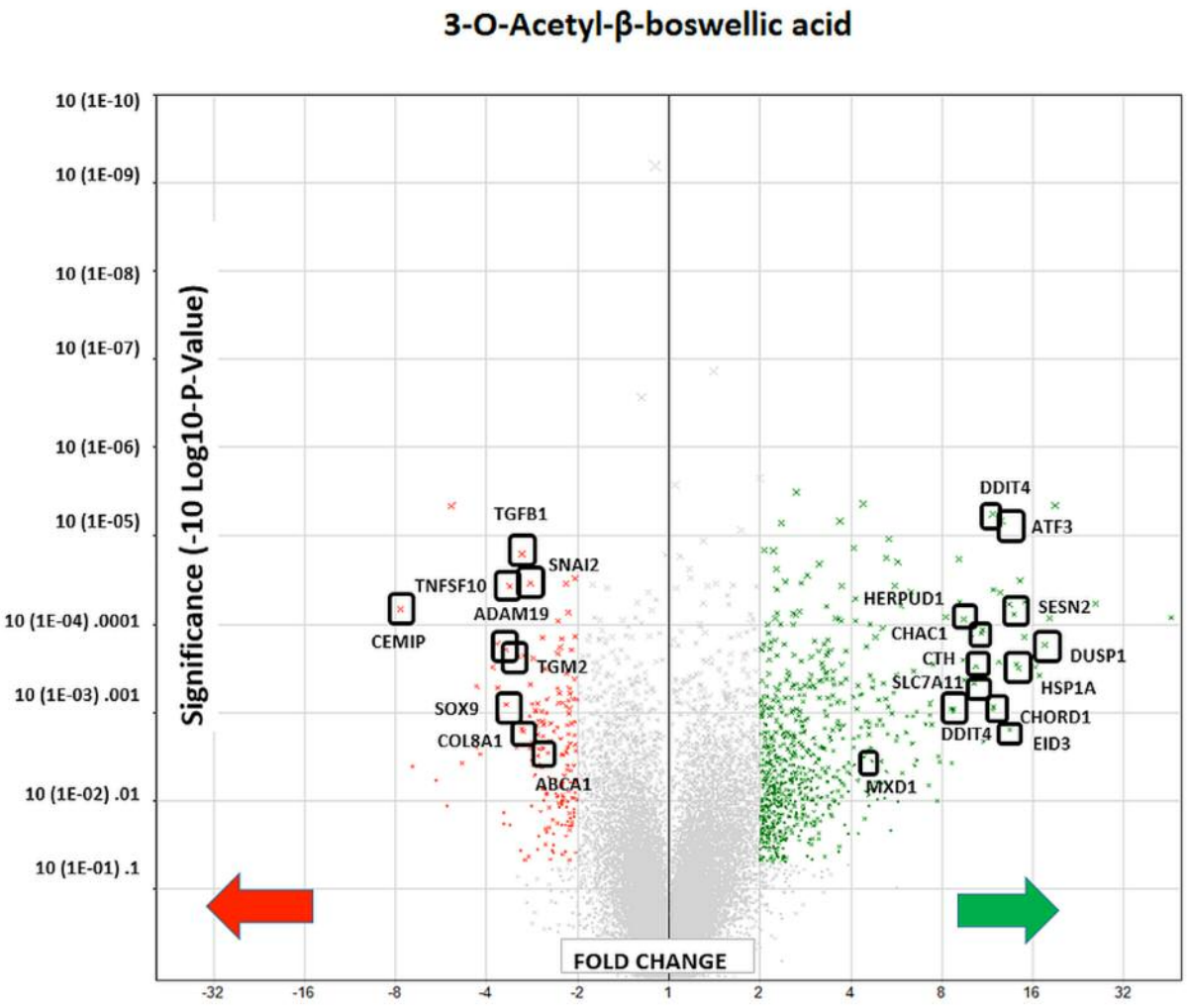

Figure 6. *WT changes in 3-OAβBA treated cells using GeneChip™ Human Gene 2.1 ST Array. 48226 transcripts tested: 931 DEGs were identified (391 up-regulated/540 down-regulated). The data are presented as a volcano Plot (fold change by significance) for whole transcriptome changes in 3-OAβBA treated MDA-MB-231 cells vs. controls, n=3. The left panel shows down-regulated genes (red)/right panel shows up-regulated genes (green): highlighting some of the top changes, also listed in Table II.*

Table II. *Largest differential shifts incurred by 3-OAβBA in MDA-MB-231 cells. The data represent signal, fold-change, p-value, gene symbol and gene description. Top mRNA Changes: Affymetrix Microarray WT Human 2.1 ST.*

Transcript	3-OAβBA	Control	Fold	ANOVA	Gene	Gene
Cluster ID	Bi-weighted AVE Signal Log2	Bi-weighted AVE Signal Log2	Change	*p*-Value	Symbol	Description
17016375	7.32	2.47	28.77	0.0001	HIST1H1T	Histone cluster 1, H1t
17114701	7.12	2.54	23.91	0.0038	CDR1	Cerebellar degeneration related protein 1
17083614	7.71	3.91	13.9	0.0002	LURAP1L	Leucine rich adaptor protein 1-like
17005573	8.39	4.6	13.88	0.0002	HIST1H2BD	Histone cluster 1, H2bd
16692603	7.32	3.53	13.77	0.0001	HIST2H2BF	Histone cluster 2, H2bf
17016379	7.07	3.35	13.17	0.0005	HIST1H2BC	Histone cluster 1, H2bc

Table II. *Continued*

Table II. *Continued*

Transcript	3-OAβBA	Control	Fold	ANOVA	Gene	Gene
Cluster ID	Bi-weighted AVE Signal Log2	Bi-weighted AVE Signal Log2	Change	*p*-Value	Symbol	Description
16756310	8.34	4.75	12.02	0.0001	TCP11L2	t-complex 11, testis-specific-like 2
16691619	7.17	3.68	11.22	0.0006	LINC00622	Long intergenic non-protein coding RNA 622
16677278	7.12	3.78	10.17	0.0001	ATF3	Activating transcription factor 3
16756202	9.71	6.41	9.8	0.0002	EID3	EP300 interacting inhibitor of differentiation 3
16692611	6.16	2.88	9.73	0.0001	HIST2H2BF	Histone cluster 2, H2bf
17006863	11.42	8.15	9.63	0.0001	HSPA1B,A	Heat shock 70kDa protein 1A;b
17002846	9.7	6.45	9.52	0.0001	DUSP1	Dual specificity phosphatase 1
16697370	7.02	3.81	9.29	0.0004	PTGS2	Prostaglandin-endoperoxide synthase 2
17052552	5.88	2.79	8.48	0.0065	MGAM2	Maltase-glucoamylase 2 (putative)
16877555	8.5	5.49	8.09	0.0002	RHOB	Ras homolog family member B
16979917	10.69	7.69	8	<0.0001	SLC7A11	Solute carrier family 7 member 11
16819325	9.36	6.37	7.96	0.0001	HERPUD1	Homocysteine-inducible, ER stress-inducible, ubi DM 1
17006881	11.44	8.48	7.78	<0.0001	HSPA1B,A	Heat shock 70kDa protein 1B; A
16670377	8.79	5.85	7.7	0.0007	HIST2H4aB	Histone cluster 2, H4b; histone cluster 2, H4a
16661544	7.71	4.78	7.64	0.0011	SESN2	Sestrin 2
16666055	7.84	4.93	7.48	0.0003	CTH	Cystathionine gamma-lyase
16960801	7.61	4.73	7.37	0.0090	PA2G4P4	Proliferation-associated 2G4 pseudogene 4
17005862	5.04	2.17	7.28	0.0055	HIST1H3H	Histone cluster 1, H3h
16743222	9.02	6.19	7.14	0.0001	CHORDC1	Cysteine and histidine rich domain containing 1
17052425	6.04	3.23	7.04	0.0020	MGAM	Maltase-glucoamylase
16888979	8.71	5.9	7.01	0.0009	NABP1	Nucleic acid binding protein 1
16705961	9.29	6.49	6.94	0.0002	DDIT4	DNA damage inducible transcript 4
16768738	8.84	6.05	6.92	<0.0001	NTN4	Netrin 4
16924602	7.28	4.52	6.75	0.0046	ADAMTS1	ADAM metallopeptidase / thrombospondin type 1 M1
16766578	6.17	3.47	6.51	0.0017	DDIT3	DNA-damage-inducible transcript 3
16967771	5.61	2.96	6.25	0.0014	CXCL8	Chemokine (C-X-C motif) ligand 8
16992467	6.59	3.97	6.13	0.0004	CREBRF	CREB3 regulatory factor
17050328	7.29	4.7	6.03	0.0003	DNAJB9	DnaJ (Hsp40) homolog, subfamily B, member 9
16761631	6.95	4.46	5.6	0.0051	DUSP16	Dual specificity phosphatase 16
17061430	7.94	5.49	5.46	0.0016	LINC01004	Long intergenic non-protein coding RNA 1004
17088116	5.42	3	5.36	0.0061	MIR4668	MicroRNA 4668
16703242	6.98	4.6	5.2	0.0005	OTUD1	OTU deubiquitinase 1
17000518	6.13	3.76	5.14	0.0016	HSPA9	Heat shock 70kDa protein 9 (mortalin)
16903897	6.39	4.05	5.06	<0.0001	NR4A2	Nuclear receptor subfamily 4, group A, member 2
16799739	7.08	4.81	4.82	0.0019	CHAC1	ChaC glutathione-specific gamma-glutamylcyclotransferase 1
17060061	7.9	5.65	4.75	0.0005	ASNS	Asparagine synthetase (glutamine-hydrolyzing)
16692632	7.89	5.65	4.72	0.0001	HIST2H2BE	Histone cluster 2, H2be
16869653	10.54	8.3	4.71	<0.0001	DNAJB1	DnaJ (Hsp40) homolog, subfamily B, member 1
16951188	5.66	3.44	4.66	0.0018	METTL6	Methyltransferase like 6
16743432	5.34	3.31	4.08	0.0018	SESN3	Sestrin 3
16859763	5.88	7.73	–3.62	0.0068	IFI30	Interferon, gamma-inducible protein 30
17075529	3.81	5.67	–3.64	0.0002	ENTPD4	Ectonucleoside triphosphate diphosphohydrolase 4
16845657	8.02	9.88	–3.64	0.0077	SLC25A39	Solute carrier family 25, member 39
17000208	3.79	5.69	–3.73	0.0023	VTRNA2-1	Vault RNA 2-1
16815310	7.86	9.79	–3.8	0.0368	TNFRSF12A	Tumor necrosis factor receptor superfamily, member 12A
16925398	5.3	7.23	–3.81	0.0064	RUNX1-IT1	RUNX1 intronic transcript 1
16866946	7.43	9.37	–3.83	0.0465	TIMM13	Translocase of inner mitochondrial mem 13 homolog (yeast)
16920671	4.86	6.81	–3.87	0.0039	PMEPA1	Prostate transmembrane protein, androgen induced 1
16921433	4.76	6.71	–3.87	0.0049	RGS19	Regulator of G-protein signaling 19
16837418	7.05	9.07	–4.06	0.0048	SOX9	SRY box 9
16726183	8.29	10.33	–4.09	0.0175	COX8A	Cytochrome c oxidase subunit VIIIA (ubiquitous)
16811638	5.65	7.75	–4.29	0.0047	SEMA7A	Semaphorin 7A, GPI membrane anchor
16828886	4.26	6.42	–4.45	0.0160	GINS2	GINS complex subunit 2 (Psf2 homolog)
16919158	5.91	8.22	–4.96	0.0032	TGM2	Transglutaminase 2
16819233	4.56	6.92	–5.12	0.0066	MT1A	Metallothionein 1A
16803754	4.95	7.8	–7.22	0.0015	CEMIP	Cell migration inducing protein, hyaluronan binding

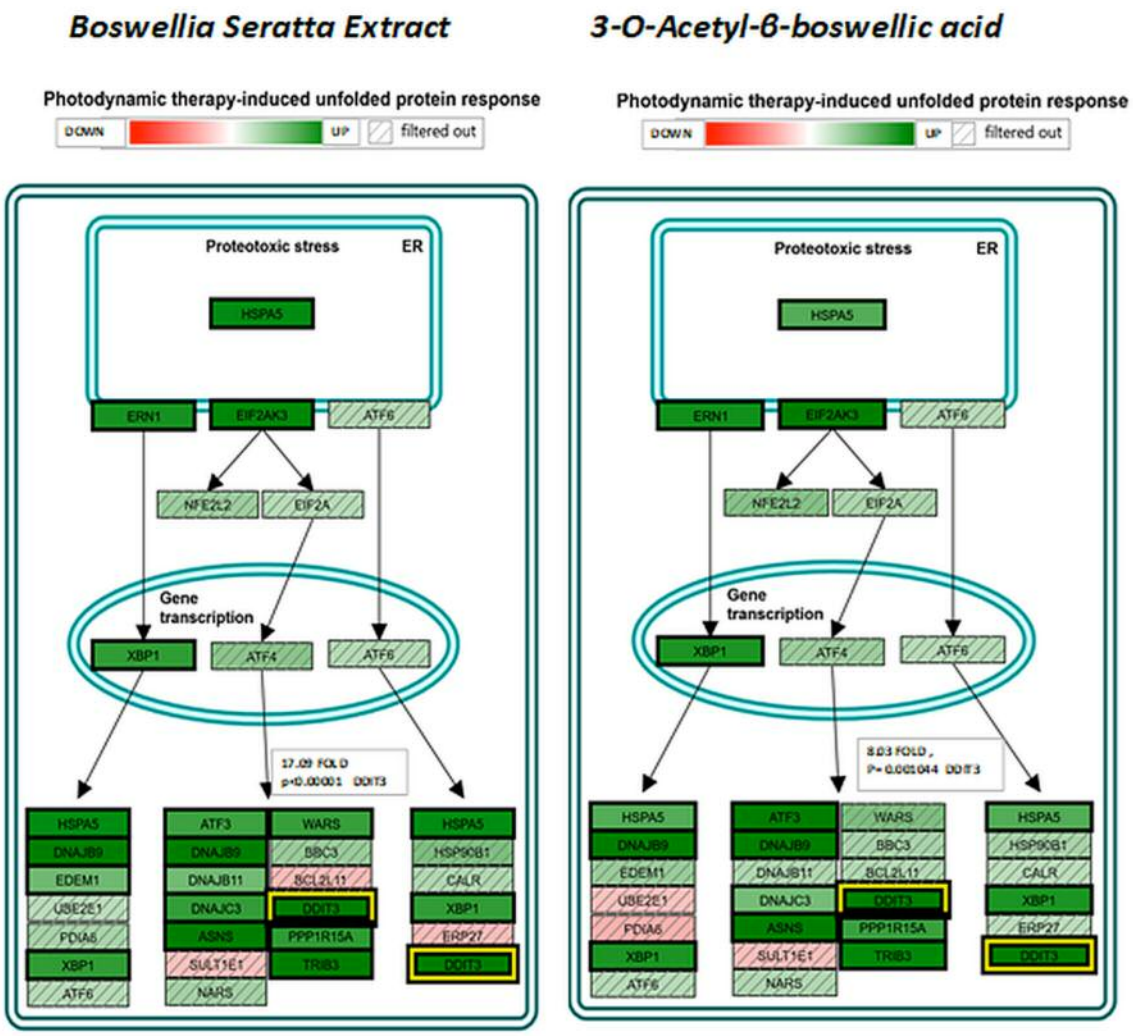

Figure 7. *Affymetrix Transcription Analysis Console/Wikipaths Correlation by Significance shows impact on Photodynamic therapy unfolded protein response by BSE and 3-3-OAβBA in MDA-MB-231 cells, with a high degree of overlap. The data represents relative fold change by intensity (green) up-regulation, (red) down-regulation with (//////) filtered out as non-significant directional changes. Highlighted in yellow is the shift in DDIT3, with values presented.*

cancer therapies (50). The data from this study show BSE and 3-OAβBA to impact several processes within the ER/UPR.

ER/UPR. If we take a look at the normal function of the ER under non-stress conditions, its main purpose is in the post-translational modification and folding of mature proteins using chaperones and foldases, which are then trafficked to the Golgi. Anything that impairs this system elicits ER stress and a UPR. This later response (ER/UPR) serves a primary means to reduce protein load by decreasing translation, and removing mis-folded proteins. This is accomplished by increasing the folding capability of the ER, and the degradation rate of damaged proteins through binding to glucose-regulated protein 78 (Bip/GRP78) (a pivotal event) in preparation for disposal through an endoplasmic reticulum-associated degradation pathway (ERAD) by the ubiquitin/proteasome pathway or alternatively, an autophagic/lysosomal pathway (51, 52).

Briefly, the ER/UPR main branches can all initiate pro-apoptotic events. These include:
[Pathway 1] protein kinase RNA-like endoplasmic reticulum kinase (PERK),
[Pathway 2] inositol-requiring enzyme-1 (IRE1), or
[Pathway 3] activating transcription factor-6 (ATF-6) (53, 54).
The effects of 3-OAβBA and BSE on the transcriptome suggests extensive up-regulation on many of these processes.

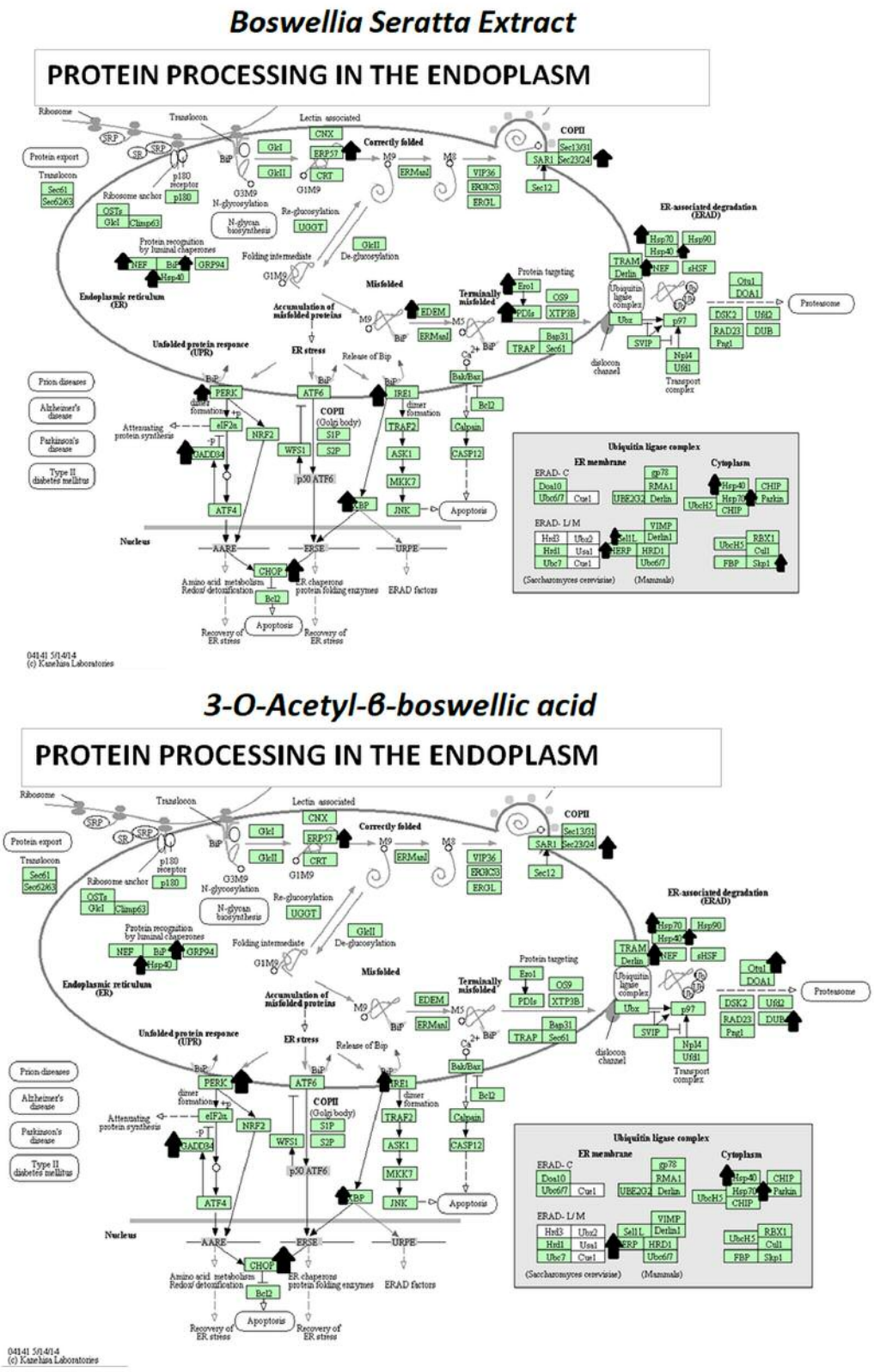

Figure 8. *DAVID Functional Annotation Bioinformatics Microarray Analysis. DAVID Bioinformatics Resources 6.8. KEGG Diagram Overlap of up-regulated transcripts in response by BSE and 3-O-Acetyl-β-boswellic acid in MDA-MB-231 cells, with a high degree of overlap. The data represents Protein Processing in the ER and up-regulated transcripts noted by an arrow.*

Table III. *Biological processes impacted by BSE-treated MDA-MB-231 cells. The data are derived from full dataset analysis using a relational database provided by geneontology.org. This service connects GO Enrichment Analysis to the analysis tool from the PANTHER Classification System, which is maintained up to date with GO annotations. The p-Value (Column 4) is the probability of seeing at least x number of genes (Column 2) out of the total n genes in the process annotated (Column 1) with greater fold enrichment score (Column 3) corresponding to relevant pathway significance impact.*

Table IIIa: GO biological process: Up-regulated by BSE	Homo sapiens - REFLIST (21002)	Genes	(fold Enrichment)	(*p*-Value)
PERK-mediated unfolded protein response	12	6	44.31	0.0001
Positive regulation of transcription from RNA polymerase II promoter in response to ER stress	12	5	36.92	0.0028
Intrinsic apoptotic signaling pathway in response to endoplasmic reticulum stress	31	8	22.87	<0.0001
Positive regulation of transcription from RNA polymerase II promoter in response to stress	25	6	21.27	0.0045
IRE1-mediated unfolded protein response	58	12	18.33	<0.0001
ER-nucleus signaling pathway	36	7	17.23	0.0020
Endoplasmic reticulum unfolded protein response	115	21	16.18	<0.0001
Response to unfolded protein	160	29	16.06	<0.0001
Cellular response to unfolded protein	121	21	15.38	<0.0001
Response to topologically incorrect protein	180	30	14.77	<0.0001
Positive regulation of response to endoplasmic reticulum stress	36	6	14.77	0.0359
Serine family amino acid metabolic process	42	7	14.77	0.0056
Cellular response to glucose starvation	37	6	14.37	0.0419
Cellular response to topologically incorrect protein	139	22	14.03	<0.0001
Regulation of response to endoplasmic reticulum stress	75	11	13	<0.0001
Response to endoplasmic reticulum stress	244	32	11.62	<0.0001
Regulation of transcription from RNA polymerase II promoter in response to stress	115	13	10.02	<0.0001
Cell redox homeostasis	73	8	9.71	0.0198
Regulation of DNA-templated transcription in response to stress	121	13	9.52	<0.0001
Intrinsic apoptotic signaling pathway	156	12	6.82	0.0026
Protein folding	237	16	5.98	0.0002
Response to starvation	173	11	5.63	0.0487
Response to toxic substance	215	13	5.36	0.0119
Cellular response to extracellular stimulus	208	12	5.11	0.0486
Cellular response to external stimulus	281	16	5.05	0.0016
Regulation of apoptotic signaling pathway	383	20	4.63	0.0002
Cellular amino acid metabolic process	313	16	4.53	0.0065
Apoptotic signaling pathway	294	15	4.52	0.0147

Analysis Type: http://www.geneontology.org/PANTHER Overrepresentation Test (release 20170413)
Annotation Version and Release Date:GO Ontology database Released 2017-07-1
Analyzed List: Up-regulated by BSE in MDA-231 Cells
Reference List: Homo sapiens (all genes in database)

Table IIIb: GO biological process: Down-regulated by BSE	Homo sapiens - REFLIST (21002)	GENES	(fold Enrichment)	(*p*-Value)
Negative regulation of epithelial cell differentiation	39	4	44.88	0.019
Mesenchymal cell differentiation	132	6	19.89	0.005
Regulation of ossification	183	6	14.35	0.034
Mesenchyme development	194	6	13.53	0.047
Animal organ morphogenesis	880	11	5.47	0.032

Pathway 1/PERK: Briefly, when proteins are misfolded in the ER, they bind to BiP/Grp78 which triggers X-box-binding protein 1 (XBP1) splicing, which then initiates PERK to phosphorylate +P (eIF2α). We found evidence of BSE not only up-regulating XBP1 +3.31, p=0.0003 (3-OAβBA), +3.04, p=0.0003 (BSE) but also PERK (EIF2AK3) +4.6 p=0.0003 (3-OAβBA) and +3.67, p<0.0003 (BSE). This active +PeIF2 α, is central to the control of downstream events which halting protein synthesis, cell cycle arrest in addition to activating ATF4, which in turn elevates ATG12, TRB3 (AKT/mTOR

Table IV. *Biological processes impacted by 3-O-Acetyl-β-boswellic acid-treated MDA-MB-231 cells. The data are derived from full dataset analysis using a relational database provided by geneontology.org. This service connects GO Enrichment Analysis to the analysis tool from the PANTHER Classification System, which is maintained up to date with GO annotations. The p-Value (Column 4) is the probability of seeing at least x number of genes (Column 2) out of the total n genes in the process annotated (Column 1) with greater fold enrichment score (Column 3) corresponding to relevant pathway significance impact.*

Table IVa: GO biological process: Up-regulated by 3-OAβBA	Homo sapiens - REFLIST (21002)	Genes Enrichment)	(fold	(*p*-Value)
PERK-mediated unfolded protein response	12	7	46.06	<0.0001
Positive regulation of transcription from RNA polymerase II promoter in response to ER stress	12	5	32.9	0.0049
Positive regulation of transcription from RNA polymerase II promoter in response to stress	25	7	22.11	0.0004
ER-nucleus signaling pathway	36	8	17.55	0.0002
Response to unfolded protein	160	23	11.35	<0.0001
Positive regulation of smooth muscle cell proliferation	74	10	10.67	0.0005
Regulation of response to endoplasmic reticulum stress	75	10	10.53	0.0005
Endoplasmic reticulum unfolded protein response	115	15	10.3	<0.0001
Response to topologically incorrect protein	180	23	10.09	<0.0001
Cellular response to unfolded protein	121	15	9.79	<0.0001
Cellular response to topologically incorrect protein	139	15	8.52	<0.0001
Regulation of smooth muscle cell proliferation	115	12	8.24	0.0004
Regulation of transcription from RNA polymerase II promoter in response to stress	115	12	8.24	0.0004
Cellular response to starvation	136	14	8.13	<0.0001
Regulation of DNA-templated transcription in response to stress	121	12	7.83	0.0006
Regulation of fat cell differentiation	113	11	7.69	0.0026
Nucleosome assembly	118	11	7.36	0.0039
Response to hydrogen peroxide	108	10	7.31	0.0139
Cellular response to nutrient levels	180	16	7.02	<0.0001
Response to starvation	173	15	6.85	0.0001
Cellular response to extracellular stimulus	208	18	6.83	<0.0001
Chromatin assembly	134	11	6.48	0.0133
Response to endoplasmic reticulum stress	244	19	6.15	<0.0001
Nucleosome organization	147	11	5.91	0.0319
Cellular response to external stimulus	281	21	5.9	<0.0001
Chromatin assembly or disassembly	154	11	5.64	0.0492
Response to reactive oxygen species	183	12	5.18	0.0437

Analysis Type: http://www.geneontology.org/PANTHER Overrepresentation Test (release 20170413)
Annotation Version and Release Date: GO Ontology database Released 2017-07-21
Analyzed List: Up-regulated by 3-OAβBA in MDA-231 Cells
Reference List: Homo sapiens (all genes in database)

Table IVb: GO biological process: Down-regulated by 3-OAβBA	Homo sapiens - REFLIST (21002)	GENES	(fold Enrichment)	(*p*-Value)
Intrinsic apoptotic signaling pathway in response to DNA damage	70	11	6.85	0.008
Positive regulation of apoptotic signaling pathway	181	17	4.09	0.014
Extracellular matrix organization	308	22	3.11	0.036
Extracellular structure organization	309	22	3.1	0.038
Response to oxidative stress	366	25	2.98	0.018
Regulation of endopeptidase activity	391	26	2.9	0.018
Regulation of apoptotic signaling pathway	383	25	2.84	0.038
Regulation of peptidase activity	418	27	2.81	0.019
Negative regulation of protein metabolic process	1105	55	2.17	0.001
Negative regulation of cellular protein metabolic process	1046	51	2.12	0.004
Negative regulation of molecular function	1161	55	2.06	0.004
Regulation of cellular component organization	2331	87	1.63	0.035

Table V. *Transcriptome miRNA changes in BSE treated MDA-MB-231 cells. The data represents cluster, signal, fold change, p-value, gene symbol, and gene targets.*

miRNA Changes: Affymetrix 4.1 mRNA Array					
Transcript	BSE	Control	Fold	ANOVA	Gene
Cluster ID	Bi-weighted AVE Signal Log2	Bi-weighted AVE Signal Log3	Change	*p*-Value	Symbol
20519591	2.11	1.09	2.03	0.00398	hsa-miR-4740-3p
20518919	5.7	6.92	-2.34	0.004005	hsa-miR-4521
20500722	3.85	5.3	-2.72	0.009182	hsa-miR-27b-5p
20501169	0.7	2.2	-2.82	0.020278	hsa-miR-34b-3p
20500786	0.96	2.28	-2.49	0.032848	hsa-miR-184
20538228	4.1	2.95	2.22	0.039779	U70D

Gene targets	
[miR-34b-3p]	[miR-184]
MET	*INPPL1*
CREB	*NFAT1*
CDK4	*AK T2*
c-MYC	*NFATC2*
BCL2	
CDK6	
MYC	
VEGFA	

inhibitor), triggering autophagy required for removal of unfolded proteins. These events are often simultaneous with the rise in C/EBP homologous protein transcription factor (CHOP)/DNA damage-inducible transcript 3, 4 or GADD153,GADD34, and ATF3 (triggering cell death) (55, 56). The data in this study show mediated effects for TRB3 [+6.3 fold, $p<0.0001$ BSE/+3.68, $p<0.0001$ 3-OAβBA] ATF3 [+12.61 fold, $p<0.0001$ BSE/+2.9, $p<0.0001$ 3-OAβBA], DDIT3 [+17.09 fold, $p<0.0001$ BSE/+8.03, $p<0.0001$ 3-OAβBA] and DDIT4 [+8.41 fold, $p<0.0001$ BSE/+11.77, $p<0.0001$ 3-OAβBA]. If CHOP driven ER stress mediated apoptosis prevails, this would drive up-regulation of death molecules (BIM, BAX, PUMA), death receptors (Tnfrsf10b/Dr5) juxtaposed to a reduction of BLC2 (anti-apoptotic molecules) (55, 57), activation of JNK and p38MAPK, rise in immediate early response genes (EGR-1), and ASK1 recruitment to IRE1-TRAF2, linking pathway 1 to the next ER/UPR stress pathway Pathway 2/ IRE1α; ERN1. The data in this study again, show consistent trends in downstream events including elevated levels of EGR-1, [+15.18 fold, $p<0.0001$ BSE/+2.48, $p<0.0001$ 3-OAβBA], TRB3 [+6.3 fold, $p<0.0001$ BSE/+3.68, $p<0.0001$ 3-OAβBA] and ATF3 [+12.61 fold, $p<0.0001$ BSE/+2.9, $p<0.0001$ 3-OAβBA].

Pathway 2/ IRE1α; ERN1: In response to unfolded proteins, IRE1α; ERN1 is cleaved by endoribonuclease activity at the 26bp intron of XBP1 (involved with pathway 1 above), which then facilitates the formation of transcription factor XBP1 mRNA, where IRE1-XBP1 can trigger recruitment of TRAF2 to the ER membrane (+ASK1 recruitment). TRAF2 is an activator of apoptosis signal-regulating kinase 1 (ASK1), which can lead to JNK mediated apoptosis. Also, this pathway can trigger ERO1α to activate the ER calcium channel inositol-1,4,5-trisphosphate receptor 1 (IP3R1) enabling activate cAMP response elements (CREs).

Pathway 3/ATF 6: Upon ER stress, ATF6 dissociates from GRP78/BiP – leaving it free to translocate to the Golgi, where it is cleaved by S1P and S2P, and its fragment released to the cytosol. ATF6 fragments can include the active 50kDa transcription factor (ATF6 p50) which translocate to the nucleus. There, ATF6 p50 and XBP1 bind ERSE promoters and up-regulate chaperones that are involved with unfolded protein response including GRP78.

ER/UPR stress mediated apoptosis and cancer drugs. Many natural products are being reported to impact the aforementioned, including a spiked rise in Grp78, CHOP with activated ER/UPR – PCD occurring through PERK, IRE1alpha and ATF6 pathways as in the case of cryptotanshinone (32) 2-(3,4-dihydroxyphenyl)ethanol (olive oil) (58) selenium (59) methylseleninic acid, sodium selenite (33) xanthohumol (hops), docosahexaenoic acid (34, 35) isochaihulactone (Nan-Chai-Hu) (36) Shikonin (Lithospermum erythrorhizon) (37) chrysin (31) curcumin (40) silibinin (41) or whole herbs such as the Chinese herbal medicine *Tu Bei Mu* (39). A number of drugs also mediate similar effects, such as steroids, platins, taxol, alkylating agents, or cancer chemicals which on the one hand block the growth of diverse cancers, and on the other hand elevate ER/UPR – PCD, associated with up-regulation of GRP78, CHOP and three UPR-associated pathways, PERK, IRE1alpha, and ATF6 (42-44, 46,

60). It is also believed that hydrogen peroxide tumor mediated cell death also corresponds to up-regulation of the PERK branch evident by +P eIF2α and the mRNA levels of activating transcription factor 4 (ATF4), C/EBP homologous (CHOP) and tribbles homolog 3 (TRB3)(61). The findings in this work, place 3-OAβBA and BSE in this category of anti-cancer agents.

While discussing all the changes in the transcriptome initiated by 3-OAβBA and BSE are beyond the scope of this paper, noteworthy is the rise in CHAC1, which is involved in the degradation of glutathione (62, 63) reported to occur in parallel to rise of ATF4-ATF3-CHOP PERK and the phosphorylation of EIF2α, where its rise creates vulnerability of cancer cells to the losses of glutathione associated with radiation and oxidative insult (64, 65) also rendering losses on glutathione detoxification systems (66).

In conclusion, we provide whole transcriptome data analysis of RNA from TNBC cells treated with 3-OAβBA and BSE. The data discussed in this publication have been deposited in NCBI's Gene Expression Omnibus and are accessible through GEO Series accession number GSE102891 located at https://www.ncbi.nlm.nih.gov/geo/query/acc.cgi?acc=GSE102891.The findings reflect a high probability of ER/UPR involvement through PERK phosphorylation of eIF2α, leading to up-regulation of ATF3, 4, TRB3, DNA damage-inducible transcript 3, 4 (CHOP) and rise in immediate early response genes. Future research will be required to determine the unique controlling factors in common between natural products and the ER/ UPR programmed death events in tumor cells.

Conflicts of Interest

The Authors wish to confirm that there are no known conflicts of interest associated with this publication and there has been no significant financial support for this work that could have influenced its outcome.

Acknowledgements

This project was supported by the National Institutes of Health, National Institute on Minority Health and Health Disparities, RCMI grant (8G12MD007582-28.) and COE grant (P20 MD006738).

References

1 Estrada AC, Syrovets T, Pitterle K, Lunov O, Buchele B, Schimana-Pfeifer J, Schmidt T, Morad SA and Simmet T: Tirucallic acids are novel pleckstrin homology domain-dependent Akt inhibitors inducing apoptosis in prostate cancer cells. Mol Pharmacol *77*: 378-387, 2010.

2 Yadav VR, Prasad S, Sung B, Gelovani JG, Guha S, Krishnan S and Aggarwal BB: Boswellic acid inhibits growth and metastasis of human colorectal cancer in orthotopic mouse model by down-regulating inflammatory, proliferative, invasive and angiogenic biomarkers. Int J Cancer *130*: 2176-2184, 2012.

3 Frank MB, Yang Q, Osban J, Azzarello JT, Saban MR, Saban R, Ashley RA, Welter JC, Fung KM and Lin HK: Frankincense oil derived from *Boswellia carteri* induces tumor cell specific cytotoxicity. BMC Complement Altern Med *9*: 6, 2009.

4 Park B, Prasad S, Yadav V, Sung B and Aggarwal BB: Boswellic acid suppresses growth and metastasis of human pancreatic tumors in an orthotopic nude mouse model through modulation of multiple targets. PLoS One *6*: e26943, 2011.

5 Ranjbarnejad T, Saidijam M, Moradkhani S and Najafi R: Methanolic extract of *Boswellia serrata* exhibits anti-cancer activities by targeting microsomal prostaglandin E synthase-1 in human colon cancer cells. Prostaglandins Other Lipid Mediat *131*: 1-8, 2017.

6 Dozmorov MG, Yang Q, Wu W, Wren J, Suhail MM, Woolley CL, Young DG, Fung KM and Lin HK: Differential effects of selective frankincense (Ru Xiang) essential oil versus non-selective sandalwood (Tan Xiang) essential oil on cultured bladder cancer cells: a microarray and bioinformatics study. Chin Med *9*: 18, 2014.

7 Lee DH, Kim SS, Seong S, Woo CR and Han JB: A case of metastatic bladder cancer in both lungs treated with korean medicine therapy alone. Case Rep Oncol *7*: 534-540, 2014.

8 Thummuri D, Jeengar MK, Shrivastava S, Areti A, Yerra VG, Yamjala S, Komirishetty P, Naidu VG, Kumar A and Sistla R: *Boswellia ovalifoliolata* abrogates ROS mediated NF-kappaB activation, causes apoptosis and chemosensitization in Triple Negative Breast Cancer cells. Environ Toxicol Pharmacol *38*: 58-70, 2014.

9 Takada Y, Ichikawa H, Badmaev V and Aggarwal BB: Acetyl-11-keto-beta-boswellic acid potentiates apoptosis, inhibits invasion, and abolishes osteoclastogenesis by suppressing NF-kappa B and NF-kappa B-regulated gene expression. J Immunol *176*: 3127-3140, 2006.

10 Zhang YS, Xie JZ, Zhong JL, Li YY, Wang RQ, Qin YZ, Lou HX, Gao ZH and Qu XJ: Acetyl-11-keto-beta-boswellic acid (AKBA) inhibits human gastric carcinoma growth through modulation of the Wnt/beta-catenin signaling pathway. Biochim Biophys Acta *1830*: 3604-3615, 2013.

11 Liu JJ, Huang B and Hooi SC: Acetyl-keto-beta-boswellic acid inhibits cellular proliferation through a p21-dependent pathway in colon cancer cells. Br J Pharmacol *148*: 1099-1107, 2006.

12 Qurishi Y, Hamid A, Sharma PR, Wani ZA, Mondhe DM, Singh SK, Zargar MA, Andotra SS, Shah BA, Taneja SC and Saxena AK: NF-kappaB down-regulation and PARP cleavage by novel 3-alpha-butyryloxy-beta-boswellic acid results in cancer cell specific apoptosis and *in vivo* tumor regression. Anticancer Agents Med Chem *13*: 777-790, 2013.

13 Kunnumakkara AB, Nair AS, Sung B, Pandey MK and Aggarwal BB: Boswellic acid blocks signal transducers and activators of transcription 3 signaling, proliferation, and survival of multiple myeloma *via* the protein tyrosine phosphatase SHP-1. Mol Cancer Res *7*: 118-128, 2009.

14 Chou YC, Suh JH, Wang Y, Pahwa M, Badmaev V, Ho CT and Pan MH: *Boswellia serrata* resin extract alleviates azoxymethane (AOM)/dextran sodium sulfate (DSS)-induced colon tumorigenesis. Mol Nutr Food Res, 2017. doi: 10.1002/mnfr.201600984. [Epub ahead of print]

15 Xue X, Chen F, Liu A, Sun D, Wu J, Kong F, Luan Y, Qu X and Wang R: Reversal of the multidrug resistance of human ileocecal adenocarcinoma cells by acetyl-11-keto-beta-boswellic acid *via* down-regulation of P-glycoprotein signals. Biosci Trends *10*: 392-399, 2016.

16 Buchele B, Zugmaier W, Estrada A, Genze F, Syrovets T, Paetz C, Schneider B and Simmet T: Characterization of 3alpha-acetyl-11-keto-alpha-boswellic acid, a pentacyclic triterpenoid inducing apoptosis *in vitro* and *in vivo*. Planta Med *72*: 1285-1289, 2006.
17 Mazzio EA and Soliman KF: *In vitro* screening for the tumoricidal properties of international medicinal herbs. Phytother Res *23*: 385-398, 2009.
18 Yazdanpanahi N, Behbahani M and Yektaeian A: Effect of boswellia thurifera gum methanol extract on cytotoxicity and p53 gene expression in human breast cancer cell line. Iran J Pharm Res *13*: 719-724, 2014.
19 Ashburner M, Ball CA, Blake JA, Botstein D, Butler H, Cherry JM, Davis AP, Dolinski K, Dwight SS, Eppig JT, Harris MA, Hill DP, Issel-Tarver L, Kasarskis A, Lewis S, Matese JC, Richardson JE, Ringwald M, Rubin GM and Sherlock G: Gene ontology: tool for the unification of biology. The Gene Ontology Consortium. Nat Genet *25*: 25-29, 2000.
20 Huang da W, Sherman BT and Lempicki RA: Systematic and integrative analysis of large gene lists using DAVID bioinformatics resources. Nat Protoc *4*: 44-57, 2009.
21 Vlachos IS, Zagganas K, Paraskevopoulou MD, Georgakilas G, Karagkouni D, Vergoulis T, Dalamagas T and Hatzigeorgiou AG: DIANA-miRPath v3.0: deciphering microRNA function with experimental support. Nucleic Acids Res *43*: W460-466, 2015.
22 Papadopoulos GL, Alexiou P, Maragkakis M, Reczko M and Hatzigeorgiou AG: DIANA-mirPath: Integrating human and mouse microRNAs in pathways. Bioinformatics *25*: 1991-1993, 2009.
23 Zhang Y, Qu X and Jiang L: An oasis in the desert of cancer chemotherapeutic resistance: The enlightenment from reciprocal crosstalk between signaling pathways of UPR and autophagy in cancers. Biomed Pharmacother *92*: 972-981, 2017.
24 Papaioannou A and Chevet E: Driving cancer tumorigenesis and metastasis through UPR signaling. Curr Top Microbiol Immunol, 2017. doi: 10.1007/82_2017_36. [Epub ahead of print]
25 Obacz J, Avril T, Le Reste PJ, Urra H, Quillien V, Hetz C and Chevet E: Endoplasmic reticulum proteostasis in glioblastoma-From molecular mechanisms to therapeutic perspectives. Sci Signal *10*: pii: eaal2323, 2017.
26 Koong AC, Chauhan V and Romero-Ramirez L: Targeting XBP-1 as a novel anti-cancer strategy. Cancer Biol Ther *5*: 756-759, 2006.
27 Le Mercier M, Lefranc F, Mijatovic T, Debeir O, Haibe-Kains B, Bontempi G, Decaestecker C, Kiss R and Mathieu V: Evidence of galectin-1 involvement in glioma chemoresistance. Toxicol Appl Pharmacol *229*: 172-183, 2008.
28 Hsiao JR, Chang KC, Chen CW, Wu SY, Su IJ, Hsu MC, Jin YT, Tsai ST, Takada K and Chang Y: Endoplasmic reticulum stress triggers XBP-1-mediated up-regulation of an EBV oncoprotein in nasopharyngeal carcinoma. Cancer Res *69*: 4461-4467, 2009.
29 Salaroglio IC, Panada E, Moiso E, Buondonno I, Provero P, Rubinstein M, Kopecka J and Riganti C: PERK induces resistance to cell death elicited by endoplasmic reticulum stress and chemotherapy. Mol Cancer *16*: 91, 2017.
30 Corazzari M, Gagliardi M, Fimia GM and Piacentini M: Endoplasmic Reticulum Stress, Unfolded Protein Response, and Cancer Cell Fate. Front Oncol *7*: 78, 2017.
31 Ryu S, Lim W, Bazer FW and Song G: Chrysin induces death of prostate cancer cells by inducing ROS and ER stress. J Cell Physiol *232*: 3786-3797, 2017.
32 Wu CF, Seo EJ, Klauck SM and Efferth T: Cryptotanshinone deregulates unfolded protein response and eukaryotic initiation factor signaling in acute lymphoblastic leukemia cells. Phytomedicine *23*: 174-180, 2016.
33 Shigemi Z, Manabe K, Hara N, Baba Y, Hosokawa K, Kagawa H, Watanabe T and Fujimuro M: Methylseleninic acid and sodium selenite induce severe ER stress and subsequent apoptosis through UPR activation in PEL cells. Chem Biol Interact *266*: 28-37, 2017.
34 Jakobsen CH, Storvold GL, Bremseth H, Follestad T, Sand K, Mack M, Olsen KS, Lundemo AG, Iversen JG, Krokan HE and Schonberg SA: DHA induces ER stress and growth arrest in human colon cancer cells: associations with cholesterol and calcium homeostasis. J Lipid Res *49*: 2089-2100, 2008.
35 Slagsvold JE, Pettersen CH, Follestad T, Krokan HE and Schonberg SA: The antiproliferative effect of EPA in HL60 cells is mediated by alterations in calcium homeostasis. Lipids *44*: 103-113, 2009.
36 Tsai SF, Tao M, Ho LI, Chiou TW, Lin SZ, Su HL and Harn HJ: Isochaihulactone-induced DDIT3 causes ER stress-PERK independent apoptosis in glioblastoma multiforme cells. Oncotarget *8*: 4051-4061, 2017.
37 Piao JL, Cui ZG, Furusawa Y, Ahmed K, Rehman MU, Tabuchi Y, Kadowaki M and Kondo T: The molecular mechanisms and gene expression profiling for shikonin-induced apoptotic and necroptotic cell death in U937 cells. Chem Biol Interact *205*: 119-127, 2013.
38 Zhang B, Han H, Fu S, Yang P, Gu Z, Zhou Q and Cao Z: Dehydroeffusol inhibits gastric cancer cell growth and tumorigenicity by selectively inducing tumor-suppressive endoplasmic reticulum stress and a moderate apoptosis. Biochem Pharmacol *104*: 8-18, 2016.
39 Xu Y, Chiu JF, He QY and Chen F: Tubeimoside-1 exerts cytotoxicity in HeLa cells through mitochondrial dysfunction and endoplasmic reticulum stress pathways. J Proteome Res *8*: 1585-1593, 2009.
40 Rivera M, Ramos Y, Rodriguez-Valentin M, Lopez-Acevedo S, Cubano LA, Zou J, Zhang Q, Wang G and Boukli NM: Targeting multiple pro-apoptotic signaling pathways with curcumin in prostate cancer cells. PLoS One *12*: e0179587, 2017.
41 Ham J, Lim W, Bazer FW and Song G: Silibinin stimluates apoptosis by inducing generation of ROS and ER stress in human choriocarcinoma cells. J Cell Physiol, 2017. doi: 10.1002/jcp.26069. [Epub ahead of print]
42 Zhang L, Hapon MB, Goyeneche AA, Srinivasan R, Gamarra-Luques CD, Callegari EA, Drappeau DD, Terpstra EJ, Pan B, Knapp JR, Chien J, Wang X, Eyster KM and Telleria CM: Mifepristone increases mRNA translation rate, triggers the unfolded protein response, increases autophagic flux, and kills ovarian cancer cells in combination with proteasome or lysosome inhibitors. Mol Oncol *10*: 1099-1117, 2016.
43 Boelens J, Lust S, Offner F, Bracke ME and Vanhoecke BW: Review. The endoplasmic reticulum: a target for new anticancer drugs. In Vivo *21*: 215-226, 2007.
44 Zanotto-Filho A, Dashnamoorthy R, Loranc E, de Souza LH, Moreira JC, Suresh U, Chen Y and Bishop AJ: Combined Gene Expression and RNAi Screening to Identify Alkylation Damage Survival Pathways from Fly to Human. PLoS One *11*: e0153970, 2016.
45 Gifford JB and Hill R: GRP78 influences chemoresistance and prognosis in cancer. Curr Drug Targets, 2017. doi: 10.2174/1389450118666170615100918. [Epub ahead of print]

46 Holtrup F, Bauer A, Fellenberg K, Hilger RA, Wink M and Hoheisel JD: Microarray analysis of nemorosone-induced cytotoxic effects on pancreatic cancer cells reveals activation of the unfolded protein response (UPR). Br J Pharmacol *162*: 1045-1059, 2011.
47 Nawrocki ST, Carew JS, Pino MS, Highshaw RA, Dunner K Jr., Huang P, Abbruzzese JL and McConkey DJ: Bortezomib sensitizes pancreatic cancer cells to endoplasmic reticulum stress-mediated apoptosis. Cancer Res *65*: 11658-11666, 2005.
48 Vanacker H, Vetters J, Moudombi L, Caux C, Janssens S and Michallet MC: Emerging Role of the Unfolded Protein Response in Tumor Immunosurveillance. Trends Cancer *3*: 491-505, 2017.
49 Ojha R and Amaravadi RK: Targeting the unfolded protein response in cancer. Pharmacol Res *120*: 258-266, 2017.
50 Cubillos-Ruiz JR, Bettigole SE and Glimcher LH: Tumorigenic and Immunosuppressive Effects of Endoplasmic Reticulum Stress in Cancer. Cell *168*: 692-706, 2017.
51 Cerezo M and Rocchi S: New anti-cancer molecules targeting HSPA5/BIP to induce endoplasmic reticulum stress, autophagy and apoptosis. Autophagy *13*: 216-217, 2017.
52 Wang J, Lee J, Liem D and Ping P: HSPA5 Gene encoding Hsp70 chaperone BiP in the endoplasmic reticulum. Gene *618*: 14-23, 2017.
53 So AY, de la Fuente E, Walter P, Shuman M and Bernales S: The unfolded protein response during prostate cancer development. Cancer Metastasis Rev *28*: 219-223, 2009.
54 Mohamed E, Cao Y and Rodriguez PC: Endoplasmic reticulum stress regulates tumor growth and anti-tumor immunity: a promising opportunity for cancer immunotherapy. Cancer Immunol Immunother *66*: 1069-1078, 2017.
55 Rozpedek W, Pytel D, Mucha B, Leszczynska H, Diehl JA and Majsterek I: The Role of the PERK/eIF2alpha/ATF4/CHOP Signaling Pathway in Tumor Progression During Endoplasmic Reticulum Stress. Curr Mol Med *16*: 533-544, 2016.
56 Cho YM, Jang YS, Jang YM, Chung SM, Kim HS, Lee JH, Jeong SW, Kim IK, Kim JJ, Kim KS and Kwon OJ: Induction of unfolded protein response during neuronal induction of rat bone marrow stromal cells and mouse embryonic stem cells. Exp Mol Med *41*: 440-452, 2009.
57 Farooqi AA, Li KT, Fayyaz S, Chang YT, Ismail M, Liaw CC, Yuan SS, Tang JY and Chang HW: Anticancer drugs for the modulation of endoplasmic reticulum stress and oxidative stress. Tumour Biol *36*: 5743-5752, 2015.
58 Guichard C, Pedruzzi E, Fay M, Marie JC, Braut-Boucher F, Daniel F, Grodet A, Gougerot-Pocidalo MA, Chastre E, Kotelevets L, Lizard G, Vandewalle A, Driss F and Ogier-Denis E: Dihydroxyphenylethanol induces apoptosis by activating serine/threonine protein phosphatase PP2A and promotes the endoplasmic reticulum stress response in human colon carcinoma cells. Carcinogenesis *27*: 1812-1827, 2006.
59 Zu K, Bihani T, Lin A, Park YM, Mori K and Ip C: Enhanced selenium effect on growth arrest by BiP/GRP78 knockdown in p53-null human prostate cancer cells. Oncogene *25*: 546-554, 2006.
60 Notte A, Rebucci M, Fransolet M, Roegiers E, Genin M, Tellier C, Watillon K, Fattaccioli A, Arnould T and Michiels C: Taxol-induced unfolded protein response activation in breast cancer cells exposed to hypoxia: ATF4 activation regulates autophagy and inhibits apoptosis. Int J Biochem Cell Biol *62*: 1-14, 2015.
61 Pierre N, Barbe C, Gilson H, Deldicque L, Raymackers JM and Francaux M: Activation of ER stress by hydrogen peroxide in C2C12 myotubes. Biochem Biophys Res Commun *450*: 459-463, 2014.
62 Bachhawat AK and Kaur A: Glutathione Degradation. Antioxid Redox Signal, 2017. doi: 10.1089/ars.2017.7136. [Epub ahead of print]
63 Kaur A, Gautam R, Srivastava R, Chandel A, Kumar A, Karthikeyan S and Bachhawat AK: ChaC2, an enzyme for slow turnover of cytosolic glutathione. J Biol Chem *292*: 638-651, 2017.
64 Crawford RR, Prescott ET, Sylvester CF, Higdon AN, Shan J, Kilberg MS and Mungrue IN: Human CHAC1 Protein degrades glutathione, and mRNA induction is regulated by the transcription factors ATF4 and ATF3 and a bipartite ATF/CRE regulatory element. J Biol Chem *290*: 15878-15891, 2015.
65 Mungrue IN, Pagnon J, Kohannim O, Gargalovic PS and Lusis AJ: CHAC1/MGC4504 is a novel proapoptotic component of the unfolded protein response, downstream of the ATF4-ATF3-CHOP cascade. J Immunol *182*: 466-476, 2009.
66 Liu Y, Hyde AS, Simpson MA and Barycki JJ: Emerging regulatory paradigms in glutathione metabolism. Adv Cancer Res *122*: 69-101, 2014.

Received August 21, 2017
Revised October 1, 2017
Accepted October 5, 2017